

## Tall-barrier terahertz quantum cascade lasers

Chun Wang I. Chan,<sup>1,a)</sup> Qing Hu,<sup>1</sup> and John L. Reno<sup>2</sup>

<sup>1</sup>*Department of Electrical Engineering and Computer Science, Massachusetts Institute of Technology, Cambridge, Massachusetts 02139, USA*

<sup>2</sup>*Center for Integrated Nanotechnologies, Sandia National Laboratories, MS 1303, Albuquerque, New Mexico 87185-1303, USA*

(Received 16 July 2013; accepted 27 September 2013; published online 11 October 2013)

A terahertz quantum cascade laser is presented in which selectively placed pure AlAs barriers are used to reduce parasitic leakage currents to the conduction band continuum. The design is demonstrated to have improved temperature performance over a regrowth of the current  $T_{\max} \sim 200$  K record holder (181 K vs. 175 K). Strangely, it fails to lase below  $\sim 70$  K, which we attribute to negative differential resistance (NDR) prior to threshold. A subsequent design using only AlAs barriers failed to lase, the reason for which we posit to be either early NDR or excessive interface roughness scattering. © 2013 AIP Publishing LLC. [<http://dx.doi.org/10.1063/1.4824878>]

Applications of terahertz quantum cascade lasers (THz QCLs) are hindered by the latter's need for cryogenic cooling, being currently limited to  $T_{\max} \sim 200$  K.<sup>1</sup> Increasing THz QCL operation temperature is therefore a crucial research goal.<sup>2</sup> One possible cause of temperature degradation is over-barrier parasitic leakage currents to the conduction band continuum. This is a known problem in mid-infrared (MIR) QCLs,<sup>3</sup> which frequently employ extremely tall conduction band barriers as a solution.<sup>3–5</sup> Inspired by the successes in MIR QCLs, we report here results on a GaAs/Al<sub>0.15</sub>Ga<sub>0.85</sub>As THz QCL in which some barriers are selectively replaced with pure AlAs to suppress parasitic leakages.

THz QCL designs using multiple Al fractions have been explored in Ref. 6, in which Monte-Carlo simulations predict that such designs yield superior gain and temperature performance. Unfortunately, experimental results did not support these predictions.<sup>7</sup> Nevertheless, removing the constraint of using only a single Al fraction per design can be reasonably hypothesized to improve performance. An important advantage of the present work over Ref. 7 is that AlAs is a stoichiometric binary material and requires no additional calibration of Al flux during growth by molecular beam epitaxy (MBE).

The structure, named NRC-V775C, is a modification of the  $T_{\max} \sim 200$  K design reported in Ref. 1. The injector barrier is replaced with a pure AlAs barrier with a thickness chosen to maintain the same injection coupling ( $2\hbar\Omega_{1/4} \sim 2.7$  meV). All other layers are adjusted to maintain roughly the same energy separations and diagonality. The injector barrier was chosen for replacement with AlAs because it is the thickest barrier. Replacement of all Al<sub>0.15</sub>Ga<sub>0.85</sub>As barriers with pure AlAs is difficult because the small subband separations in THz QCLs would require some sub-monolayer barriers. For comparison, the design of Ref. 1 was regrown in the same MBE machine as structure NRC-V775A. The bandstructures for NRC-V775C and NRC-V775A are shown in Figure 1, calculated using a 3-band  $\mathbf{k} \cdot \mathbf{p}$  code with  $\mathbf{k} \cdot \mathbf{p}$  parameters taken from Ref. 8.

Following the recommendations of Ref. 8, discontinuities of 0.149 and 1.050 eV are used for GaAs/Al<sub>0.15</sub>Ga<sub>0.85</sub>As and GaAs/AlAs interfaces, respectively (the device of Ref. 1 was designed using 0.135 eV for GaAs/Al<sub>0.15</sub>Ga<sub>0.85</sub>As).<sup>9</sup>

A tall injector barrier introduces additional confinement for high energy subbands, which should raise their energy and therefore reduce thermionic emission to continuum. It also increases the dwell time for continuum electrons in each QCL module; this promotes thermalization down to the conduction band edge and reduces the likelihood of hot electron injection into the subsequent module. Finally, it reduces tunneling of electrons from subbands 2 and 3 into the subsequent module.

NRC-V775C (wafer number VB0487) and NRC-V775A (wafer number VB0486) were grown by MBE with 230 and 227 cascaded modules, respectively, resulting in a total thickness of  $\sim 10 \mu\text{m}$  in each case. A 50 nm (100 nm) Si-doped GaAs contact layer is grown above (below) the  $10 \mu\text{m}$  thick active region, doped to  $n = 5 \times 10^{18} \text{ cm}^{-3}$  (the 100 nm contact layer is later removed by wet-etching). A 400 nm Al<sub>0.55</sub>Ga<sub>0.45</sub>As etch-stop layer underlies the entire growth. Laser ridges were clad in Ta(10 nm)/Au metal-metal waveguides and dry etched in 1:3:16 Cl<sub>2</sub>:SiCl<sub>4</sub>:Ar using an inductively coupled plasma (ICP) etcher. The fabricated devices were cleaved, indium soldered ridge side-up on a copper mount, wire-bonded, and mounted on the cold stage of a pulsed tube cryocooler.

Experimental results are shown in Figures 2 and 3. The low temperature lasing frequency is lower than expected from a one-module simulation. Although the prediction of lasing frequency in THz QCLs is nontrivial,<sup>10</sup> this is consistent with a strong, coherent coupling between the injector subband and the upper laser level, which pushes down the energy of the latter. In Figure 2, the increase of the threshold current as temperature rises is clearly slower in NRC-V775C, consistent with a reduction in parasitic leakages. Surprisingly, NRC-V775C did not lase below  $\sim 70$  K. Despite this, NRC-V775C lased up to 181 K in pulsed mode, whereas NRC-V775A lased up to 175 K. Both structures are inferior to the original  $\sim 200$  K structure in Ref. 1. NRC-V775C was overgrown by 1.2%, and NRC-V775A was

<sup>a)</sup>Electronic mail: icwchan@mit.edu

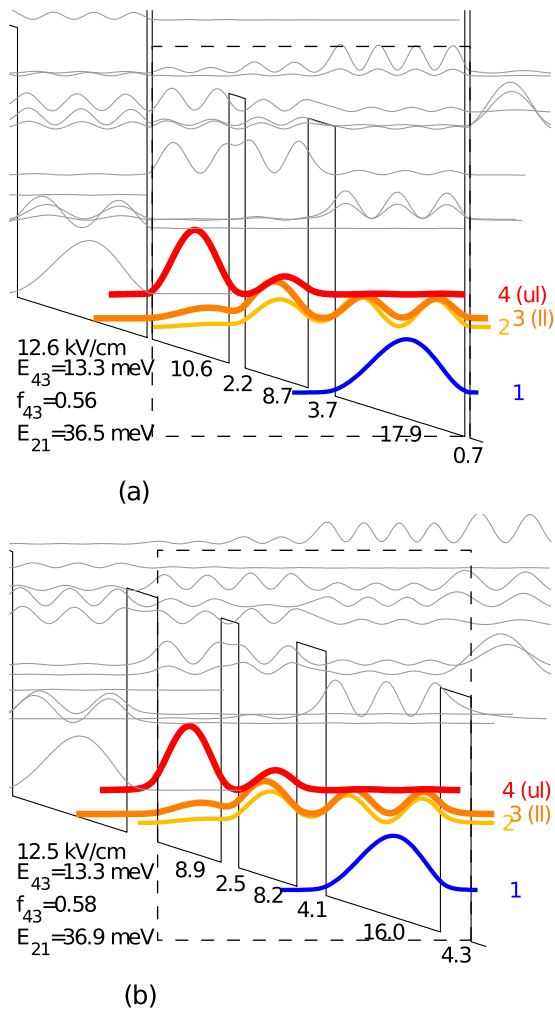


FIG. 1. Band diagrams for (a) NRC-V775C and (b) NRC-V775A. Layers are marked by their thicknesses in nm, and one module is boxed in each case. In both cases, the middle 5 nm of the widest well is doped to  $6 \times 10^{15} \text{ cm}^{-3}$ .

undergrown by 1.8%, so growth differences may be at play; we note in Figure 2(b) that the optical output starts decreasing prior to the negative differential resistance feature (NDR) near the design bias. This is absent in the original structure and may point to slight growth problems. Part of the drop in  $T_{\text{max}}$  may also be caused by the use of Ta/Au waveguides instead of Ta/Cu,<sup>11</sup> or incomplete removal of the top-contact. The latter would be consistent with Ref. 1, in which different samples with intact doping layers and Ti/Au waveguides lased up to 176 and 180 K.

Rather than something exotic like DX centers<sup>12</sup> or indirect barrier states associated with the AlAs barriers, we hypothesize that the failure to lase below  $\sim 70$  K is due to the occurrence of NDR just before the threshold. This is known to harm the performance of THz QCLs, especially three well designs of this type which can suffer from voltage instabilities.<sup>13</sup> Although the extraction couplings for NRC-V775C and NRC-V775A are designed to be identical, NRC-V775C was designed with a slightly taller barrier height for  $\text{Al}_{0.15}\text{Ga}_{0.85}\text{As}$  barriers ( $2\hbar\Omega_{23} \sim 4.9$  meV was targeted, but  $2\hbar\Omega_{23} \sim 5.5$  meV if calculated using 135 meV barriers). Consequently, its extraction barrier is thinner (3.7 nm instead of 4.1 nm), which results in a stronger interaction between the injector of one QCL module and phonon well excited

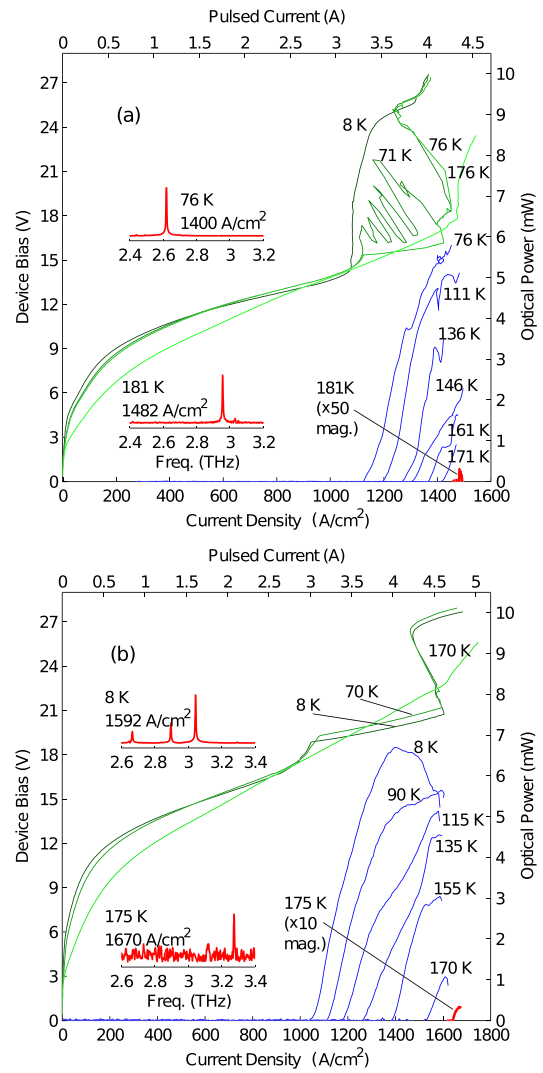


FIG. 2. Experimental light-current-voltage (LIV) and spectral data for (a) NRC-V775C ( $1.96 \text{ mm} \times 150 \mu\text{m} \times 10 \mu\text{m}$  ridge) and (b) NRC-V775A ( $1.92 \text{ mm} \times 150 \mu\text{m} \times 10 \mu\text{m}$  ridge). In (a), the 71 K IV is rough due to the intermittent onset of lasing.

state of the next (the intermediate resonance described in Ref. 13). Furthermore, low lasing frequency may be consistent with an injector barrier that is electronically thinner than expected, either due to error in growth thickness or barrier

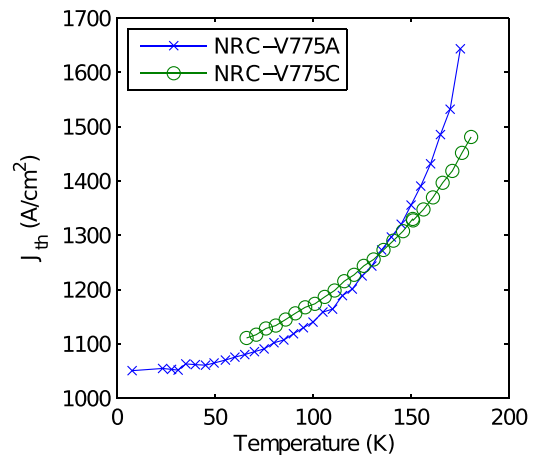


FIG. 3. Comparison of threshold current rise between NRC-V775C and NRC-V775A.

height. This would exacerbate the aforementioned parasitic. That said, it remains unclear why the lasing is so thoroughly eliminated, whereas the devices of Ref. 13 lased despite the presence of an early NDR.

NRC-V775C also has a lower maximum current density ( $J_{\max}$ ) than NRC-V775A. The natural interpretation is that increased interface roughness scattering is dephasing carrier injection into the upper laser level. But if this is the case, then one expects reduced transport due to stimulated emission and hence lower optical power. This is not apparent from Figure 2 in which the measured powers for NRC-V775C and NRC-V775A are similar. Although uncertainties in light collection efficiency hamper a direct comparison of the  $LIs$  in Figure 2, the similar power levels do suggest that the lower  $J_{\max}$  could possibly be from a reduction in parasitic currents rather than a reduction in stimulated emission due to increased dephasing.

Encouraged by the better performance of NRC-V775C over NRC-V775A, we further attempted a three-well resonant phonon active region with all AlAs barriers, shown in Figure 4(a). A very diagonal lasing transition is employed, as a vertical transition would require excessively thin barriers. The structure, OWI230T, was similarly grown and processed (except that ridges were wet etched), but failed to lase. The

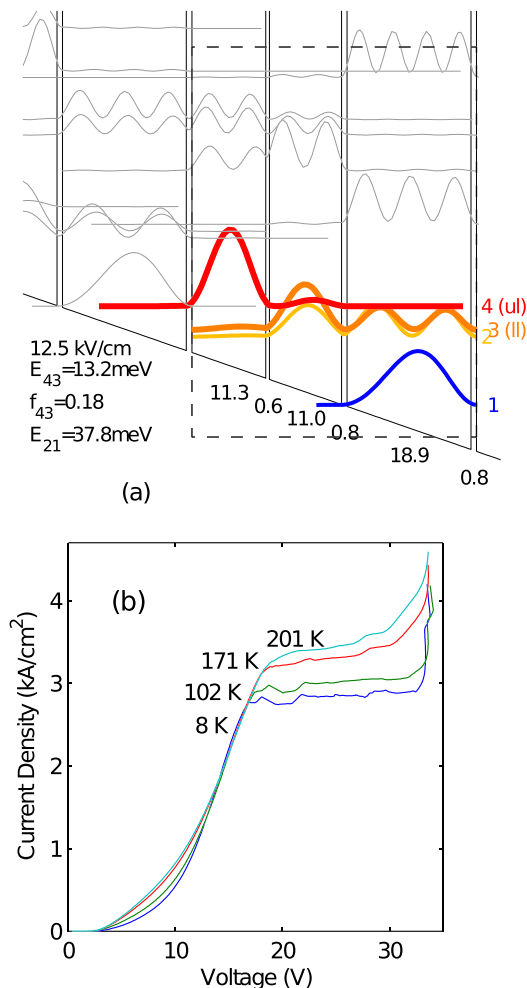


FIG. 4. OWI230T (a) band diagram and (b) experimental  $IVs$  ( $1.32 \text{ nm} \times 100 \text{ }\mu\text{m} \times 10 \text{ }\mu\text{m}$  ridge). Layers in (a) are marked by their thicknesses in nm, and one module is boxed; the middle 4.8 nm of the widest well is doped to  $2.5 \times 10^{17} \text{ cm}^{-3}$ .

$IVs$  are presented in Figure 4(b), which shows an NDR feature persisting up to  $\sim 170 \text{ K}$ . If this NDR feature is due to the same intermediate resonance, it may be that early NDR prevents lasing at any temperature in this structure. On the other hand, we speculate that OWI230T may also have failed due to excessive interface roughness scattering associated with the thin AlAs barriers. The importance of interface roughness scattering for THz QCLs has been theoretically predicted<sup>14</sup> and is further supported by recent experimental results on interface roughness scattering in nominally symmetric active regions.<sup>15</sup> From Fermi's golden rule, interface roughness scattering should scale roughly as the conduction band discontinuity squared, so switching from  $\text{Al}_{0.15}\text{Ga}_{0.85}\text{As}$  to pure AlAs should result in much greater scattering. That said, vertical correlations between the interfaces in such thin barriers should reduce the rates somewhat,<sup>16</sup> and the golden rule may not be applicable to barriers so thin that they might host voids.<sup>17</sup> Furthermore, the unavoidable monolayer fluctuation of the MBE growth will result in a large fractional fluctuation of barrier thickness (the thinnest barrier in Fig. 4(a) is only 2 monolayers thick), yielding a significant level broadening. This result from a highly diagonal QCL would be consistent with the results of Ref. 18, in which the barrier Al fraction was systematically increased for a vertical QCL design; when increased to  $\text{Al}_{0.45}\text{Ga}_{0.55}\text{As}$ , the design similarly failed to lase.

In conclusion, we demonstrate that the selective placement of pure AlAs barriers may be helpful in improving the temperature performance of THz QCLs. However, the possible reduction of leakage currents afforded by large discontinuity barriers must be balanced against an increased interface roughness scattering. Based on the present findings and the results of Refs. 15 and 18, the uniform use of tall barriers may generate too much interface roughness scattering for robust lasing to occur.

The work at the Massachusetts Institute of Technology was supported by the National Aeronautics and Space Administration and the National Science Foundation. The work at Sandia was performed, in part, at the Center for Integrated Nanotechnologies, a U.S. Department of Energy, Office of Basic Energy Sciences user facility. Sandia National Laboratories is a multiprogram laboratory managed and operated by Sandia Corporation, a wholly owned subsidiary of Lockheed Martin Corporation, for the U.S. Department of Energy National Nuclear Security Administration under contract DE-AC04-94AL85000.

<sup>1</sup>S. Fatholouloumi, E. Dupont, C. Chan, Z. Wasilewski, S. Laframboise, D. Ban, A. Mátyás, C. Jirauschek, Q. Hu, and H. C. Liu, *Opt. Express* **20**, 3866 (2012).

<sup>2</sup>B. S. Williams, *Nat. Photonics* **1**, 517 (2007).

<sup>3</sup>V. Ortiz, C. Becker, H. Page, and C. Sirtori, in *Proceedings of the 12th International Conference on Molecular Beam Epitaxy* [J. Cryst. Growth **251**, 701 (2003)].

<sup>4</sup>Y. Bai, N. Bandyopadhyay, S. Tsao, E. Selcuk, S. Slivken, and M. Razeghi, *Appl. Phys. Lett.* **97**, 251104 (2010).

<sup>5</sup>D. Botez, J. C. Shin, S. Kumar, L. J. Mawst, I. Vurgaftman, and J. R. Meyer, *Opt. Eng.* **49**, 111108 (2010).

<sup>6</sup>A. Matyas, R. Chashmahcharagh, I. Kovacs, P. Lugli, K. Vijayaraghavan, M. A. Belkin, and C. Jirauschek, *J. Appl. Phys.* **111**, 103106 (2012).

<sup>7</sup>M. A. Belkin, K. Vijayaraghavan, A. Vizbaras, A. Jiang, F. Demmerle, G. Boehm, R. Meyer, M. C. Amann, A. Matyas, R. Chashmahcharagh, P. Lugli, C. Jirauschek, and Z. R. Wasilewski, *Proc. SPIE* **8640**, 864014 (2013).

- <sup>8</sup>I. Vurgaftman, J. R. Meyer, and L. R. Ram-Mohan, *J. Appl. Phys.* **89**, 5815 (2001).
- <sup>9</sup>The motivation for using 149 meV for V775C was to be consistent with the parameters for the AlAs/GaAs used in Ref. 8. In retrospect, this was a bad idea, and we should have used a consistent barrier height for the 15% Al barriers in both designs. A better controlled test is planned.
- <sup>10</sup>T. Liu, K. E. Lee, and Q. J. Wang, *Phys. Rev. B* **86**, 235306 (2012).
- <sup>11</sup>M. A. Belkin, J. A. Fan, S. Hormoz, F. Capasso, S. P. Khanna, M. Lachab, A. G. Davies, and E. H. Linfield, *Opt. Express* **16**, 3242 (2008).
- <sup>12</sup>P. M. Mooney, *J. Appl. Phys.* **67**, R1 (1990).
- <sup>13</sup>S. Fatholouloumi, E. Dupont, Z. R. Wasilewski, C. W. I. Chan, S. G. Razavipour, S. R. Laframboise, S. Huang, Q. Hu, D. Ban, and H. C. Liu, *J. Appl. Phys.* **113**, 113109 (2013).
- <sup>14</sup>T. Kubis, C. Yeh, P. Vogl, A. Benz, G. Fasching, and C. Deutsch, *Phys. Rev. B* **79**, 195323 (2009).
- <sup>15</sup>C. Deutsch, H. Detz, T. Zederbauer, A. M. Andrews, P. Klang, T. Kubis, G. Klimeck, M. E. Schuster, W. Schrenk, G. Strasser, and K. Unterrainer, *Opt. Express* **21**, 7209 (2013).
- <sup>16</sup>S. Tsujino, A. Borak, E. Muller, M. Scheinert, C. V. Falub, H. Sigg, D. Grutzmacher, M. Giovannini, and J. Faist, *Appl. Phys. Lett.* **86**, 062113 (2005).
- <sup>17</sup>F. Carosella, R. Ferreira, G. Strasser, K. Unterrainer, and G. Bastard, *Phys. Rev. B* **82**, 033307 (2010).
- <sup>18</sup>T.-T. Lin, L. Ying, and H. Hirayama, in *Proceedings of the 36th International Conference on Infrared, Millimeter and Terahertz Waves (IRMMW-THz)*, 2011, pp. 1–2.